the singularities in either plane by the subscript zero, one obtains from Eq. (1)

$$x_0 = 2\pi k \qquad k = 0, \pm 1, \pm 2, \ldots$$

$$y_0 = \cosh^{-1}\left(\frac{1}{e}\right) = \pm\ln\left[\frac{1 + (1 - e^2)^{1/2}}{e}\right]$$

as singular points in the E plane and

$$u_0 = k \qquad k = 0, \pm 1, \ldots$$

$$v_0 = \pm\frac{1}{2\pi}\left\{\ln\left[\frac{1 + (1 - e^2)^{1/2}}{e}\right] - (1 - e^2)^{1/2}\right\} \qquad (3)$$

as critical points in the τ plane.

Clearly the singular points of the E plane are those points the real parts of which are integer multiples of 2π, lying on the two horizontal lines at a distance y_0 above and below the real (x) axis. The critical points of the τ plane are located similarly at a distance v_0 above and below the real (u) axis. In addition to this doubly infinite set, the point at infinity of each plane is a nonisolated singularity.

Thus the region of regularity in the E plane is a strip parallel to the real axis and bounded by two lines formed by two sets of singular points. The height, $2y_0$, of this strip depends on the value of e. For $e = 1$ it is zero, and no region of regularity exists. For $e = 0$ the height is infinite. For $0 < e < 1$, a limited region of regularity exists. The corresponding region of regularity in the τ plane is bounded by the images of the horizontal lines $y_0 = \text{const}$. These images are arcs going through the critical points v_0, as can be seen from Fig. 1. It may be mentioned that uniqueness is achieved by representation on the Riemann surface, e.g., Refs. 2 and 3.

Now, an analytic function always can be expanded in a Taylor series in its region of regularity. Let E be expanded in a Taylor series about a real time point τ_1, as in (2). This expansion will converge only in the region that is inside the circle of convergence about the chosen point t_1/T. The radius of this circle is the distance between the real time point t_1/T on the u axis, about which the expansion is made, and the singularity nearest to this point. Any real time point between perigee and apogee might be taken. The distance, v_0, of the singularities from the real time axis was given in (3) as a function of e. Therefore, the circle of convergence depends on the eccentricity (e) as well as on the chosen time point (t_1) about which the eccentric anomaly (E) is expanded.

Figure 2 shows the radius of convergence $R(t_1/T)$, which is greatest for an expansion at apogee ($t_1/T = \frac{1}{2}$) and smallest for an expansion at perigee ($t_1/T = 0$). Thus $v_0 \leqslant R \leqslant (v_0^2 + \frac{1}{4})^{1/2}$. This limitation of the radius of convergence, $R(t_1/T)$, covers all expansions about any real time point, t_1, during one period, T, of revolution. Figure 3 shows the radius of convergence as a function of the eccentricity, e, applied to expansions at perigee and at apogee. At other points the radius of convergence is between the values shown in the figure.

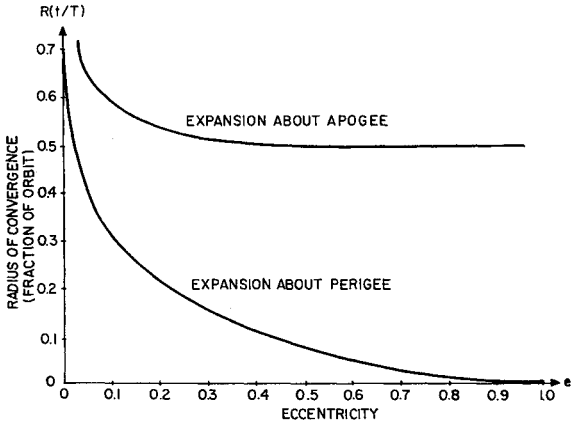

Fig. 3 Limiting values of radius of convergence

These considerations for the two-body problem emphasize the importance of investigating the analytic character of a function, in particular its region of regularity. The forementioned results indicate that a Taylor expansion must be used cautiously, especially about points near perigee of an elliptical orbit with great eccentricity. For example, when $e = 0.9$, the expansion at perigee converges only for a time interval $|\Delta t| = 0.005\ T$. Such a case occurs at injection into an earth-moon orbit, although this becomes a three-body problem.

References

[1] Moulton, F. R., *An Introduction to Celestial Mechanics* (The Macmillan Co., New York, 1959), Chap. V, pp. 165–169.

[2] Wintner, A., *Analytical Foundations of Celestial Mechanics* (Princeton University Press, Princeton, N. J., 1947), Chap. IV, pp. 212–222.

[3] Cherry, T. M., "On Kepler's equation," Proc. Cambridge Phil. Soc. 51, 81–91 (1955).

Graphical Evaluation Of the Trade-Off between Specific Impulse and Density

MORTON A. KLOTZ*
Aerojet-General Corporation, Azusa, Calif.

GORDON[1] has shown that the relative effects of propellant specific impulse I_s and density in a volume-limited vehicle may be evaluated by the equation

$$\Omega = I_s(\rho/\rho_0)^K \qquad (1)$$

where ρ is the density of the propellant, ρ_0 the density of a reference propellant, K a fraction between 0 and 1.0 calculated from the design parameters of a given vehicle, and Ω is defined as the "effective specific impulse."

The parameter K is not a constant; for a given stage it depends on the weight of the higher stages and therefore on the density of the propellant in the higher stages. Exact values of K are difficult to calculate, and it is better to calculate burnout velocities and ranges if precise results are needed for a given vehicle. Nevertheless, Eq. (1) is useful for preliminary propellant evaluation in propellant development programs. For this purpose it is satisfactory to use the K values given by Gordon for an ideally staged volume-limited vehicle with propellant mass fractions of 0.9 in each stage and a stage ratio of 3 (see Table 1).

The usefulness of Eq. (1) is enhanced by plotting Ω semilogarithmically against K, as in Fig. 1. Since

$$\log\Omega = K\log(\rho/\rho_0) + \log I_s \qquad (2)$$

such a plot yields a straight line of slope $\log(\rho/\rho_0)$ and intercept I_s. Values of Ω for any value of K between 0 and 1.0 thus are obtained by drawing a straight line between the I_s on the left ($K = 0$) and $I_s(\rho/\rho_0)$ on the right ($K = 1.0$). In such a plot, a propellant with $\rho = \rho_0$ appears as a horizontal

Received by IAS December 3, 1962; presented at the AIAA Summer Meeting, Los Angeles, Calif., June 17–20, 1963. Information contained herein was developed for the U. S. Government. The U. S. Government may publish such information at any time. A similar plot for the related equation $\Omega = I_s\rho^K$ was used in an earlier, unpublished work by L. J. Gordon, to whom the author is grateful for helpful advice and suggestions.

* Assistant Senior Chemist, Solid Propellant Research Operations.

Table 1 K values for propellant evaluation

First stage	Second stage	Third stage	∞ stage
0.70	0.36	0.25	0.15

Table 2 I_s and ρ for three hypothetical propellants

Propellant	I_s, sec	ρ, g/cm³
A) low I_s, high ρ	268	1.85
B) high I_s, low ρ	280	1.60
C) references	275	1.70

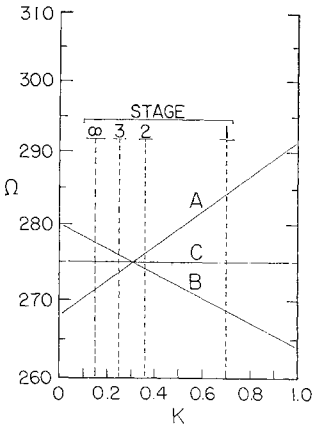

Fig. 1 Graphical propellant selection

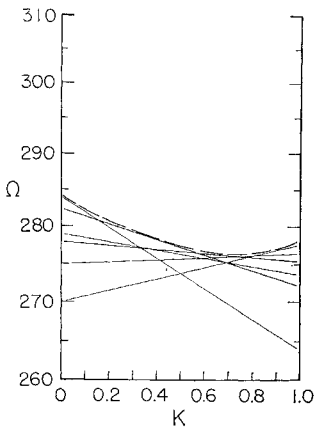

Fig. 2 Upper performance limits for a given type of propellant

line, a propellant with $\rho > \rho_0$ gives a line with a positive slope, and a propellant with $\rho < \rho_0$ gives a line with a negative slope.

Figure 1 shows the relative merits for each of the stages for three hypothetical propellants. Their specific impulses and densities are given in Table 2.

It is readily apparent that propellant A is the best of the three for the first and second stages, despite the fact that it has the lowest I_s. Propellant B is best only for the third stage, despite its high I_s. All three propellants would serve equally well for a stage with $K = 0.31$. Figure 1 also shows that, although the effect of density is smaller the higher the stage, density must be considered even for an ∞ stage.

These charts also can be used to select the optimum propellant composition or mixture ratio for each stage. The effective specific impulse Ω may vary with composition for a given type of solid propellant as shown in Fig. 2. The straight lines define an envelope showing the performance limits for this type of propellant; the optimum composition for each stage can be approximated by interpolation.

Reference

[1] Gordon, L. J., "Trade-off between propellant specific impulse and density," Aerospace Eng. **20**, 12–13, 27 (November 1961).

Direct Nonlinear Stability Analysis of Keplerian Orbital Motion

IRVING MICHELSON*
Illinois Institute of Technology, Chicago, Ill.

THE practical interest in and usefulness of Keplerian orbits is bound up inextricably with their positive stability characteristics: ubiquitous small forces and deviations that never can be accounted fully do not alter totally the character of the idealized motion. Viewing these disturbance motions as oscillatory perturbations superimposed on a basic orbit is frequently justified by the convenience, although it is strictly more accurate to consider that each disturbance gives rise to an altogether new orbit. The customary "first-approximation stability" analysis performed in this manner not only is tedious in cases of practical interest but also suffers from the more serious objection of being sometimes totally misleading.[1] The modern form of ideas first formulated by H. Poincaré permits the investigation of the stability of orbital motion in a rigorous and yet eminently practical fashion.

It is a familiar elementary exercise to be found in textbooks on dynamics to show that circular orbits possess first-approximation stability against small disturbances when an inverse-square force field is assumed. The conclusion is based on the known character of solutions of a familiar differential equation that only approximately describes the disturbance motion. For actual elliptic orbits of nonzero eccentricity, on the other hand, the same techniques lead to Mathieu equations and a problem of so much greater difficulty that none of the standard treatises contain its discussion. On purely physical qualitative grounds the omission can be excused, since the property established for a circular orbit seems plausible also for slightly eccentric ellipses, at least. For problems of satellite attitude control, however, in which librations and orbital oscillations occur and interact in near-resonance with each other, more accurate results are needed.[2] It is shown how a Liapunov function can be constructed from the energy integral of orbital motion, and hence stability is proved. An essential feature is that the conclusion does not depend on the nature of the solutions of the relevant differential equations (or even some approximation to these); the rigorous nonlinear equations themselves furnish the required results directly.

Orbital motion is specified by a pair of second-order ordinary differential equations, one of which is immediately integrable and introduces the area parameter h:

$$r - r\dot{\theta}^2 = -G/r^2$$

$$r^2\dot{\theta} = h$$

(A common notation is employed, r,θ denoting plane polar position coordinates of the satellite centroid, dots denoting time derivatives, and G denoting the constant of earth-gravitation). The corresponding energy integral per unit mass is

$$E = [(\dot{r}^2 + r^2\dot{\theta}^2)/2] - (G/r)$$

Consider a "basic" orbit $R(t)$, $\vartheta(t)$, and superposed on it a disturbed motion, the whole being given by

$$r = R + \rho$$

$$\theta = \vartheta + \varphi$$

where ρ, $\dot{\rho}$, and $\dot{\varphi}$ are small perturbations, and simplify the

Received January 3, 1963.

* Professor of Mechanical Engineering; also Visiting Professor at the Institut des Specialités Industrielles de Nancy, Université de Nancy, France, during Spring Semester 1963. Member AIAA.